Nanoscale Research Letters
a SpringerOpen Journal

NANO EXPRESS Open Access

Heterogeneous nanofluids: natural convection heat transfer enhancement

Fakhreddine Segni Oueslati[1], Rachid Bennacer[2*]

Abstract

Convective heat transfer using different nanofluid types is investigated. The domain is differentially heated and nanofluids are treated as heterogeneous mixtures with weak solutal diffusivity and possible Soret separation. Owing to the pronounced Soret effect of these materials in combination with a considerable solutal expansion, the resulting solutal buoyancy forces could be significant and interact with the initial thermal convection. A modified formulation taking into account the thermal conductivity, viscosity versus nanofluids type and concentration and the spatial heterogeneous concentration induced by the Soret effect is presented. The obtained results, by solving numerically the full governing equations, are found to be in good agreement with the developed solution based on the scale analysis approach. The resulting convective flows are found to be dependent on the local particle concentration ϕ and the corresponding solutal to thermal buoyancy ratio N. The induced nanofluid heterogeneity showed a significant heat transfer modification. The heat transfer in natural convection increases with nanoparticle concentration but remains less than the enhancement previously underlined in forced convection case.

Introduction

The existence of convection in double-diffusive systems, in which heat and salt diffuse at a different rate, was first recognised in the late 1950 s. Since then, this phenomenon has been studied extensively due to the fact that its importance has been recognised in many fields such as geophysics, astrophysics, ocean physics and industrial processes [1-4]. The first study concerning double diffusion in a binary fluid seems to be that of Nield [5]. Relying on linear stability theory, the onset of motion in an initially motionless, stable concentration and stratified horizontal fluid layer heated from below was predicted by this author. This cross-effect regarding the Rayleigh-Bénard convection dealing with the bifurcation and the possible change in the critical thresholds (i.e. transitional Rayleigh number from conductive to convective motion) was also considered on the same period by Veronis [6]. All the above studies are concerned with the effect of the regular diffusion of each component (heat and salt) on convection. However, in a wide variety of natural and industrial situations, besides the usual diffusion, cross-diffusion between the two agents may also be important. This phenomenon, known as the Soret effect, has been relatively less studied despite its importance for a fluid layer of a binary mixture (convection and stability). In recent studies, the problem of the double thermo-diffusion effects that occurs under natural convection in fluid or porous media was studied; see for example Bennacer et al. [7]

During the past ten years, a new class of fluids made up of metal nanoparticles in suspension in a liquid, called nanofluids, has appeared. Nanofluids are composed of nanoparticles that (size in general <100 nm) are suspended in a base fluid, as water or an organic solvent [8-10]. The formation of extremely stable colloidal systems with very tiny settling is a characteristic feature of some nanofluids, the stability of the suspension is naturally achieved by electrostatic stabilisation by adjusting the pH [11]. The presence of nanoparticles causes a significant modification of thermal properties of the resulting mixture; in particular, nanofluid viscosity and thermal conductivity increase with particle volume fraction. Although the increase in thermal conductivity is a very important interest, there are also increases in the average temperature of nanofluids compared to that of base fluid and that because of the specific heat of nanofluids, which decreases compared to that of base fluid [12,13]. The abnormal rise of the thermal

* Correspondence: rachid.bennacer@dgc.ens-cachan.fr
[2]ENS-Cachan Dpt GC/LMT, 61, Av du Président Wilson 94235 Cachan Cedex, France.
Full list of author information is available at the end of the article

conductivity in comparison with the pure fluid [14], especially for low particle concentrations, is not totally understood today. Some assumptions are based on particle deposition on the surface resulting in the formation of nano fins [15]. There are a many recent studies that report experimental measurements of thermophysical properties of nanofluids, including specific heat, thermal conductivity and viscosity; some recent reports include [16-19]. There has been great attention in nanofluids generated by a variety of applications, ranging from laser-assisted drug delivery to electronic chip cooling.

Some previous research works were mainly concerned with heat transfer and properties of these fluids, see Choi [20], Eastman et al. [21], Maïga et al. [22] and Wang and Mujumdar [23]. The natural convection of nanofluids deserves more attention in light compared to forced convection [24-26]. Recently, linear stability analysis, employed model incorporates the effects of Brownian motion and thermophoresis, for the onset of natural convection in a horizontal nanofluid layer [27]. For vertical layer it was underlined the existence of an optimal particle volume concentration of 2% [28,29], which maximises heat transfer.

The aim of this article is to study the increase of heat transfer taking into account both the variation of thermal conductivity and viscosity in the governing equations when using nanofluids for different types of metallic particles such as Al2O3, TiO2 and Cu. Indeed, for the modelling is as realistic as possible, we considered the Soret effect and the heterogeneity of concentration due to crossed effect.

Governing equations

In this investigation, convection within a two-dimensional vertical cavity filled by an incompressible Newtonian binary fluid (Figure 1) is studied. All boundaries of the cavity considered are impermeable; the top and bottom boundaries are assumed adiabatic whilst the other vertical ones are kept at uniform but different constant temperatures. The gravity acts in the negative direction (y).

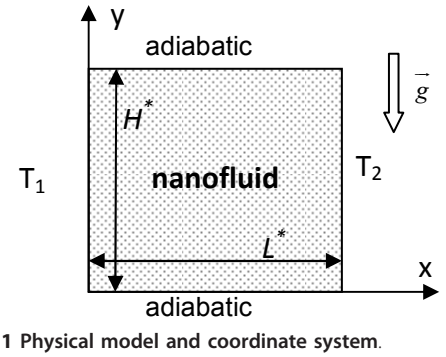

Figure 1 Physical model and coordinate system.

In this study, the heterogeneous nanofluid is considered and induced by the Soret-Ludwig effect. The nanofluid (binary mixture with diffusion coeffeicient D , see [30]) is modelled as an incompressible fluid possessing an initial uniform particle concentration C_0^* and constant physical properties except for the density, which varies with temperature and concentration according to the Boussinesq's approximation as follows:

$$\rho = \rho_0 \left[1 - \beta_T \left(T^* - T_0^*\right) - \beta_S \left(C^* - C_0^*\right)\right] \quad (1)$$

where ρ_0 is the reference fluid density at temperature and concentration $(T^*, C^*) = (T_0^*, C_0^*)$, β_T and β_S are, respectively, the thermal and solutal expansion coefficients, respectively. The microscopic mass flux, taking into account the Soret effect, is given by:

$$\vec{J}^* = -\rho\, D\left(\nabla C^* + a D_T/D\; C_0^*\left(1 - C_0^*\right)\nabla T^*\right) = 0 \quad (2)$$

the Soret effect is taken into account if $\alpha = 1$, or ignored if $a = 0$.

The derivation of the coupled governing equations, under their dimensionless form, has been based on the reference quantities for length, velocity, temperature and concentration differences given by cavity height H^*, υ/H^*, $\Delta T^* = T_1^* - T_2^*$ and $\Delta C^* = -C_0^*\left(1 - C_0^*\right) Sr \Delta T^*$.

The dimensionless variables (without *) are as follows:

$$(x, y) = (x^*, y^*)/H^*, \vec{V} = \vec{V}^*/(\upsilon/H^*), P = P^* H^{*2}/\rho\upsilon^2, \theta = \frac{(T^* - T_0^*)}{\Delta T^*} \text{ and } \phi = \frac{(C^* - C_0^*)}{\Delta C^*}$$

The dimensionless governing equations for, respectively, mass, momentum, energy and concentration are written as:

$$\nabla \cdot \vec{V} = 0 \quad (3)$$

$$\left(\vec{V} \cdot \vec{\nabla}\right)\vec{V} = -\vec{\nabla}P + \vec{\nabla}\left(\mu^r \vec{\nabla}\vec{V}\right) + Gr_T\,(\theta + N\phi)\,\vec{k} \quad (4)$$

$$\vec{V} \cdot \vec{\nabla}\theta = \frac{1}{Pr}\frac{1}{(\rho C_p)^r}\vec{\nabla} \cdot \left(\lambda^r \vec{\nabla}\theta\right) \quad (5)$$

$$\vec{V} \cdot \vec{\nabla}\phi = \frac{1}{Sc}\vec{\nabla} \cdot \left(\vec{\nabla}\phi - a\vec{\nabla}\theta\right) \quad (6)$$

The heat transfer is characterised by the Nusselt number, which is based on the reference diffusive heat flux: $q_{ref} = \lambda_f\, \Delta T^*/H^*$

With the exception of the cavity aspect ratio that does not appear explicitly in the equations, but remains indeed a key parameter of the problem, one can notice that the present problem is governed by the thermal Rayleigh number, R_T, the solutal to thermal buoyancy ratio, N, the Prandtl number, Pr, the Lewis number, Le

and a (for Soret effect occurrence). These parameters are defined as:

$$R_T = \frac{g\,\beta_T \Delta T^* H^{*3}}{\alpha \upsilon}, \quad N = \frac{\beta_S \Delta C^*}{\beta_T \Delta T^*} = , \quad a = 0 \text{ or } 1$$
$$Pr = \frac{\upsilon}{\alpha}, \quad Le = \frac{\alpha}{D}, \quad A = \frac{L^*}{H^*} \tag{7}$$

It is noted that the thermal coefficient, β_T, is usually a positive quantity. On the other hand, the solutal coefficient β_S can be positive ($N > 0$) or negative ($N < 0$). For $N > 0$, the thermal and solutal boundary forces are both destabilizing, i.e. the two buoyancy components make aiding contributions, whilst for $N < 0$, they make opposing contributions. In the present nanofluide study we have weak concentration but strong buoyancy forces wich is similar to the classical binary mixtures [31].

The controlling thermo-physical properties are the nanofluid to base fluid ratio of thermal conductivity $\lambda^r = \lambda_{nf}/\lambda_f$, and viscosity ratio $\mu^r = \mu_{nf}/\mu_f$. These characteristics are functions of the nanofluid mixture used and furthermore, space dependent due to the possible heterogeneity of nanoparticles concentration. The subscripts f, nf and r refer, respectively, to the base fluid, the nanofluid (effective properties) and relative nanofluid/base fluid ratio of the physical quantity under consideration

The dimensionless thermal, concentration and hydrodynamic boundary conditions are as follows:

$$x = 0 \; T = 1; \quad \frac{\partial C}{\partial x} = a\frac{\partial T}{\partial x} \tag{8 - a}$$

$$x = A \; T = 0; \quad \frac{\partial C}{\partial x} = a\frac{\partial T}{\partial x} \tag{8 - b}$$

$$\text{on the solid border } u = v = 0 \tag{8 - c}$$

The local heat (mass) transfer on the wall is characterised by the local Nusselt (Sherwood) number defined as:

$$Nu = \lambda^r \frac{\partial \theta}{\partial x} \text{ and } Sh = \frac{\partial \phi}{\partial x} \tag{9}$$

The average number along the active wall is given by $\overline{M} = \int_0^1 M \, dy$ ($M = Nu$ or Sh).

In the above equations, Nu represents, as usual, the heat transfers across the walls of the cavity resulting from the combined action of convection and conduction. However, because the walls of the cavity are impermeable, Sh does not have its usual significance. Here, it is rather related to the concentration distribution within the cavity induced by the Soret effect (taken into account for $\alpha = 1$, or ignored, i.e. $a = 0$) and by natural convection.

Numerical method and validation

In order to numerically solve the governing equations, a control volume approach is used. Central differences are used to approximate the advection-diffusion terms, i.e. the scheme is second-order accurate in space. By spatial integration over control volumes, the governing equations are converted into a system of algebraic equations. The latter are solved by a line-by-line iterative method, which is combined with a sweeping technique over the integration domain along x- and y-axes and a tri-diagonal matrix inversion algorithm. The SIMPLER algorithm is employed to solve the equations in a form of primitive variables. Non-uniform grids are used in the program, allowing fine grid spacing near the two horizontal walls. The convergence criteria are based on the conservation of mass, momentum, energy and species, and this is on both global and local basis.

Primarily considered a restrictive case of such a model that is the classical natural convection case for which, both influence due to particle volume fraction and Soret effect are considered negligible. Figure 2 shows the thermal and flow structure as obtained for two particular Rayleigh numbers, $R_T = 10^4$ and 10^5, the values of the stream function at the cavity centre are also given for comparison. Such a structure appears 'conventional' and similar to results reported in the literature [32,33].

A comparison of our numerical data with results from the literature and for these test cases is shown in Table 1. The agreement between our results and others can be qualified as quite satisfactory since the relative maximum deviation was found to be 4%. It is worth noting that due to a clear lack of nanofluids data, it was not possible to validate our mathematical model against experimental data for the specific case of natural convection using nanofluids in a cavity. We do firmly believe that the above agreement may give a confident assessment regarding our mathematical modelling as well as the numerical method adopted.

To ensure that the results are mesh-size independent, different non-uniform $n_y \times n_x$ meshes (where n_y and n_x represent, respectively, the node numbers in the vertical and horizontal directions), namely 41^2 and 81^2, were thoroughly tested. The difference between results given by those grids was less than 1% for Nu, Sh and Ψ_c numbers. Hence, most of the calculations presented in this article were performed using an $n_y \times n_x = 61^2$ grid. Such a grid system possesses very fine meshes near all boundaries. The solution was carried out for a validation test case with $Pr = 0.71$ in a narrow channel flow for a range of controlling parameters. The converged solution achieved with all absolute residues of the governing

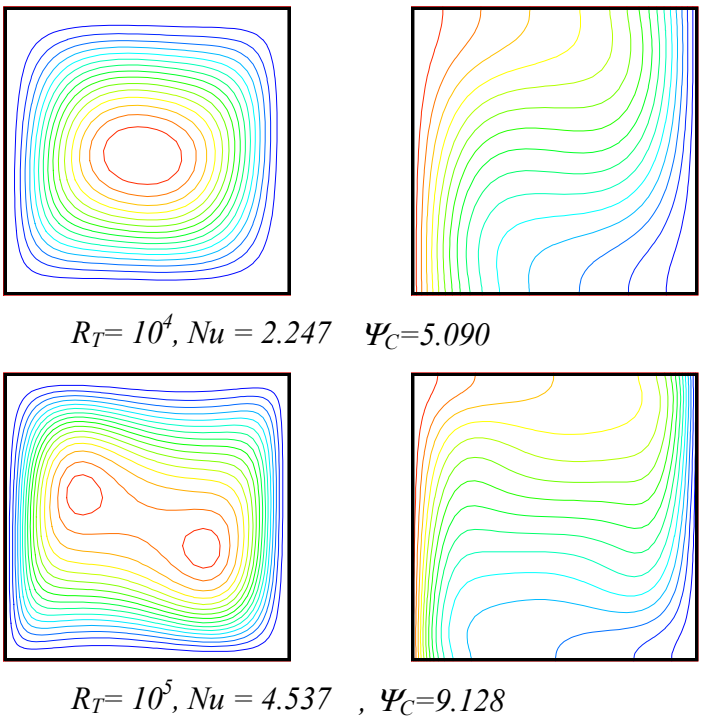

Figure 2 Dynamic and thermal fields in the case of classical natural convection (without particles and Soret effect, *Pr* = 0.71).

equations is less than 10^{-7}. All numerical results presented hereafter are obtained with parameters $A = 1$, $Pr = 6.2$, $Le = 3$ and $Sr = 2\%$.

With regard to the effective nanofluid properties, they were evaluated using the following classical relations already known for a two-phase mixture. In the following equations, p and ϕ, refer to the particles and particle volume fraction, respectively. The effective density and specific heat of the nanofluid can be estimated on the physical principle of the mixture rule as:

$$\rho_{\mathrm{nf}} = (1-\varphi)\rho_{\mathrm{f}} + \varphi\rho_{\mathrm{P}} \qquad (10-\mathrm{a})$$

$$(\rho C_p)_{\mathrm{nf}} = (1-\varphi)(\rho C_p)_{\mathrm{f}} + \varphi(\rho C_p)_{\mathrm{P}} \qquad (10-\mathrm{b})$$

Table 1 Flow intensity in the centre of the cavity versus literature results (*Pr* = 0.7, *A* = 1, ϕ = 0, *Sr* = 0, *N* = 0)

Authors:		Our results	Leal et al. [40]	Sai et al. [41]	de Vahl Davis [33]
R_T					
10^3	Ψ_C	1.136	1.175	-	1.174
	Nu_{moy}	1.117	1.118	1.130	1.117
10^4	Ψ_C	5.000	5.073	-	5.071
	Nu_{moy}	2.246	2.248	2.289	2.238
10^5	Ψ_C	9.010	9.112	-	9.111
	Nu_{moy}	4.533	4.562	4.687	4.509

The viscosity of the nanofluid can be estimated with the existing relations for the two-phase mixture. Drew and Passman [34] introduced Einstein's formula for evaluating the effective viscosity of fluids containing a dilute suspension of small rigid spherical particles, as follows:

$$\mu^{\mathrm{r}} = \mu_{\mathrm{nf}}/\mu_{\mathrm{f}} = 1 + 2.5\varphi \qquad (11)$$

This formula is restricted for low particle volume fraction, under 5%. Brinkman [35] proposed the following extension to the Einstein's formula:

$$\mu^{\mathrm{r}} = (1-\varphi)^{-2.5} \qquad (12)$$

Many other relations of effective viscosity of two-phase mixtures exist in the literature. Each relation has its own limitation and application. Some complex behaviour of nanofluids has also been observed by Keblinski et al. [36]. Unfortunately, results reveal that Brinkman's formula underestimates the few experimental data present in literature. In this study, we choose the following polynomial approximation based on experimental data [16,17,37], for water-Al_2O_3 nanofluid):

$$\mu^{\mathrm{r}} = 1 + 7.3\varphi + 123\varphi^2 = \mu_{\mathrm{nf}}/\mu_{\mathrm{f}} \qquad (13)$$

Many experimental researches focussed on nanofluids thermal conductivity, but all of them get different results for the same nanofluid, because of various other

parameters influencing this thermal property (concentration, shape and size of particles, dispersants used and particle agglomeration). In this study, we have adopted the Hamilton and Crosser's [38] formula in the case of spherical particles:

$$\lambda^{r} = \frac{\lambda_{nf}}{\lambda_f} = \frac{1 + 2\lambda_f/\lambda_P + 2\left(1 - \lambda_f/\lambda_P\right)\varphi}{1 + 2\lambda_f/\lambda_P - \left(1 - \lambda_f/\lambda_P\right)\varphi} = 1 + \frac{3\left(1 - \lambda_f/\lambda_P\right)\varphi}{1 + 2\lambda_f/\lambda_P - \left(1 - \lambda_f/\lambda_P\right)\varphi} \quad (14)$$

Results and discussion

In this article, despite the lack of experimental results, we use the relative specific heat capacity $(\rho C_p)^r$, which is the most realistic in the physical sense that the relative density, which multiplies the relative specific heat $(\rho^r)(C_p)^r$ which is used by several authors. Indeed, this differentiation is crucial since it greatly affects the results, which is illustrated in Figure 3a. Indeed, the comparison clearly shows that the relative specific heat capacity $(\rho^r)(C_p)^r$ continues to grow with the particle fraction of nanofluid, in the case of classical formulation, when it decreases slightly for $(\rho C_p)^r$.

As mentioned before, both viscosity and thermal conductivity increase and specific heat capacity decreases with particle concentration (Figure 4).

Based on the definition of the Nusselt number (Equation 7), the heat transfer in the case of homogeneous nanofluid is given by:

$$Nu = 0.14 \times \lambda^{r} \times R_{Tnf}^{0.305} \quad (15)$$

where

$$R_{Tnf} = \frac{g\beta\Delta T^{*}H^{*3}\rho_{nf}\left(\rho C_p\right)_{nf}}{\mu_{nf}\lambda_{nf}} = R_T\frac{\rho^{r}\left(\rho C_p\right)^{r}}{\mu^{r}\lambda^{r}}$$

$$Nu = 0.14 \times \lambda^{r}\left(R_T\frac{\left(\rho C_p\right)^{r}}{\lambda^{r}\mu^{r}/\rho^{r}}\right)^{0.305} \text{ where for } \phi = 0 \text{ it}$$

recovers the pure fluid case $Nu_{\varphi=0} = 0.14 \times R_T^{0.305}$ and the relative nanofluid heat transfer is given by:

$$Nu^{r} = \frac{Nu}{Nu_{\phi=0}} = \lambda^{r}\left(\frac{\rho^{r}\left(\rho C_p\right)^{r}}{\lambda^{r}\mu^{r}}\right)^{0.305} = \left(\lambda^{r}\right)^{0.695}\left(\frac{\rho^{r}\left(\rho C_p\right)^{r}}{\mu^{r}}\right)^{0.305} \quad (16)$$

This expression illustrates well the evolution of the relative natural convection heat transfer to the pure fluid case. The second group functions only of the particle volume fraction and the relative nanoparticles-to-base fluid viscosity and conductivity (see Equations 13 and 14), and the relative density and heat capacity are given below:

$$\rho^{r} = \frac{\rho_{nf}}{\rho_f} = (1 - \varphi) + \varphi\frac{\rho_P}{\rho_f} \quad (17)$$

$$\left(\rho C_p\right)^{r} = \frac{\left(\rho C_p\right)_{nf}}{\left(\rho C_p\right)_f} = (1 - \varphi) + \varphi\frac{\left(\rho C_p\right)_P}{\left(\rho C_p\right)_f} \quad (18)$$

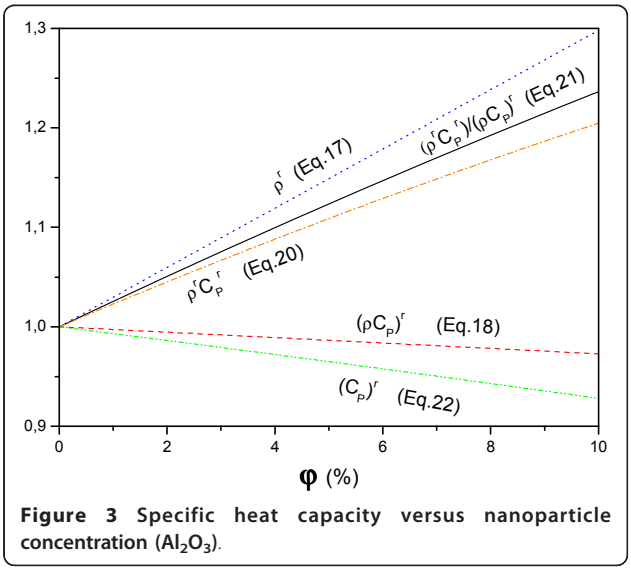

Figure 3 Specific heat capacity versus nanoparticle concentration (Al_2O_3).

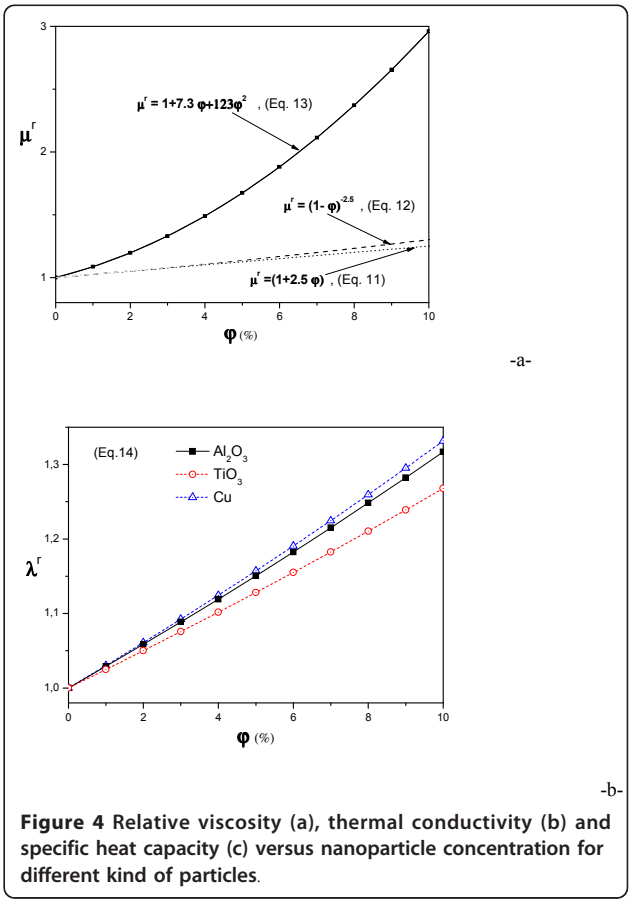

Figure 4 Relative viscosity (a), thermal conductivity (b) and specific heat capacity (c) versus nanoparticle concentration for different kind of particles.

$$\left(\rho C_p\right)_{\mathrm{nf}} - \rho_{\mathrm{nf}} C_{p_{\mathrm{nf}}} = \varphi\,(1-\varphi)\left(\rho_{\mathrm{f}} - \rho_{\mathrm{p}}\right)\left(C_{p_{\mathrm{f}}} - C_{p_{\mathrm{p}}}\right)$$

$$\Delta\left(\rho C_p\right)^{\mathrm{r}} = \frac{\left(\rho C_p\right)_{\mathrm{nf}} - \rho_{\mathrm{nf}} C_{p_{\mathrm{nf}}}}{\rho_{\mathrm{f}} C_{p_{\mathrm{f}}}} = \varphi\,(1-\varphi)\,\frac{\left(\rho_{\mathrm{f}} - \rho_{\mathrm{p}}\right)}{\rho_{\mathrm{f}}}\,\frac{\left(C_{p_{\mathrm{f}}} - C_{p_{\mathrm{p}}}\right)}{C_{p_{\mathrm{f}}}}$$

Let's define $\Delta\rho^{\mathrm{r}} = (\rho_{\mathrm{f}} - \rho_{\mathrm{p}})/\rho_{\mathrm{f}}$ and $\Delta C_p{}^{\mathrm{r}} = \left(C_{p_{\mathrm{f}}} - C_{p_{\mathrm{p}}}\right)/C_{p_{\mathrm{f}}}$

$$\Delta\left(\rho C_p\right)^{\mathrm{r}} = \varphi\,(1-\varphi)\,\Delta\rho^{\mathrm{r}}\Delta C_p{}^{\mathrm{r}} \tag{19}$$

$$\rho^{\mathrm{r}} C_p{}^{\mathrm{r}} = \left(\rho C_p\right)^{\mathrm{r}} - \varphi\,(1-\varphi)\,\Delta\rho^{\mathrm{r}}\Delta C_p{}^{\mathrm{r}} \tag{20}$$

$$\frac{\rho^{\mathrm{r}} C_p{}^{\mathrm{r}}}{\left(\rho C_p\right)^{\mathrm{r}}} = 1 - \frac{\varphi\,(1-\varphi)\,\Delta\rho^{\mathrm{r}}\Delta C_p{}^{\mathrm{r}}}{\left(\rho C_p\right)^{\mathrm{r}}} \tag{21}$$

and

$$C_p{}^{\mathrm{r}} = \left[\left(\rho C_p\right)^{\mathrm{r}} - \varphi\,(1-\varphi)\,\Delta\rho^{\mathrm{r}}\Delta C_p{}^{\mathrm{r}}\right]/\rho^{\mathrm{r}} \tag{22}$$

The effect of the particle volume fraction on the heat transfer is shown on Figure 5. The same figure exposed a comparison between the classical homogeneous nanofluid model and the heterogeneous nanofluid model. We note, for both homogeneous and heterogeneous as well as the analytical solution, there is a maximum particles concentration above which the heat transfer begins to decrease. In fact the increase of nanofluid viscosity increases the friction, so the flow rate decreases which in turn induces a diminution of heat transfer. On the other hand, an increase of nanofluid thermal conductivity would necessarily enhance the heat transfer. So, it is important to discuss which of these two effects influences most the heat transfer?

Figure 5 shows also, for the classical homogeneous nanofluid model case, that the numerical and analytical results are in good agreement and the maximum

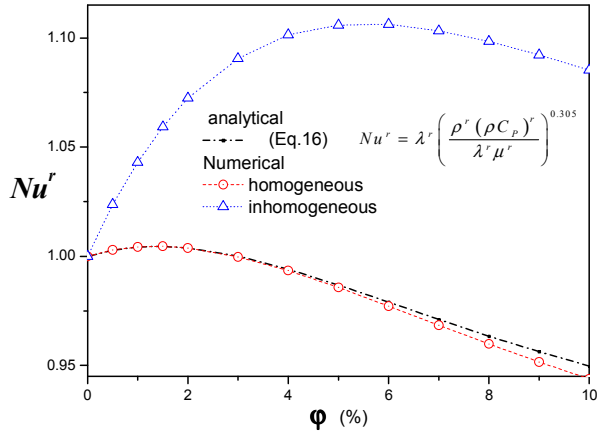

Figure 5 Nanoparticle fraction effect on heat transfer (a = 0, A = 1, $R_{\mathrm{T}} = 10^5$).

Nusselt is reached for particle volume fraction of 2%. Nevertheless, for the case of the heterogeneous fluid model, we can note that the Nusselt is more enhanced and reach a maximum for particle volume fraction of 5%. In fact, the considered thermodiffusion affects clearly the heat transfer and the flow.

When the Soret effect is considered, the nanoparticle concentration within the fluid is spatial dependant (heterogeneous fluid). Such heterogeneity induces a strong non-linear effect as the conductivity, viscosity and heat capacity and solutal buoyancy became spatial-dependant. This explains the strong coupling between the flow, the heat transfer (dependent on the flow and local thermal conductivity) and the concentration which, indeed, is also dependent on both the flow and thermal fields.

Figure 6 shows a comparison between homogeneous (plotted by dashed lines) and heterogeneous (plotted by solid lines) cases on streamlines (on the left), isotherms (at the middle) and isoconcentrations (on the right) using the same nanoparticles Al_2O_3. The figure demonstrates that a single circulation cell is formed in the clockwise direction for all values of Rayleigh numbers. One can observe that the separation caused by the Soret effect clearly shows the importance of the heterogeneity of the nanoparticle concentration in the cavity. Such a spatial heterogeneity causes, in turn, a relatively important modification of the thermal field, which can modify the heat transfer rate by as much as 10%. It is worth noting that many previous results do not take into account the buoyancy forces effect caused by this heterogeneous distribution of particle concentration. Our results from Figure 6 obviously show that such heterogeneity of nanoparticle concentration induces extra buoyancy forces and would modify the momentum equilibrium. Also, Figure 6 illustrates an example of the resulting dynamic, thermal and species fields as well as the important changes related to the adding temperature and concentration effects.

The effect of the flow intensity on the optimum value of particle volume fraction observed previously is illustrated on Figure 7. For comparison and discussion purpose, the reference Nu for the base fluid is, i.e. fluid without particles, (ϕ = 0). As usual, Nu increases with R_{T}. The variation of the relative Nusselt number Nu^{r} (nanofluid to base fluid) with respect to the particle volume fraction for different R_{T} is represented in Figure 7. The relative Nusselt number increases in the diffusive regime (low Rayleigh number, $R_{\mathrm{T}} < 10^3$) as it is directly dependent on the apparent thermal conductivity. The relative heat transfer (i.e. nanofluid to base fluid) illustrates a decrease for higher Rayleigh number and is a direct consequence of the reference increase illustrated by Figure 7. These results show that the heat transfer is mainly conductive for low value of R_{T}. For intermediate

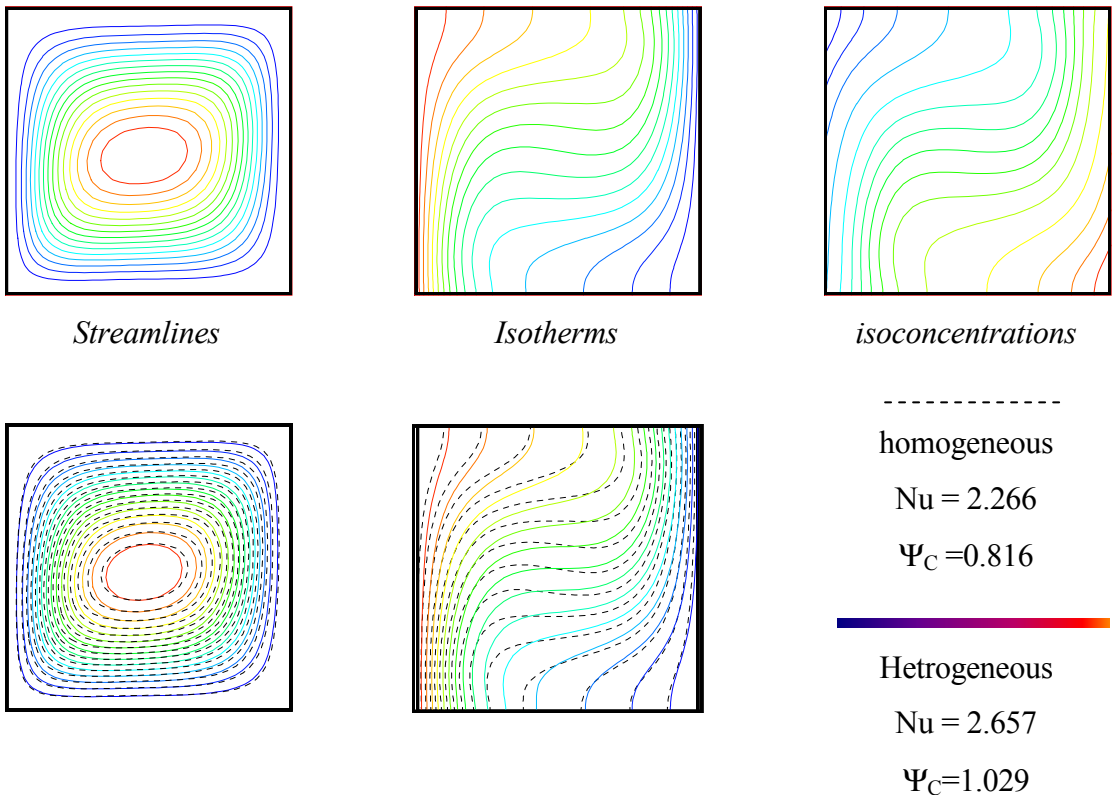

Figure 6 Dynamic, thermal and concentration fields for homogeneous (plotted by dashed lines) and heterogeneous (plotted by solid lines) cases ($R_T = 10^4$, *Pr* = 6.2, *Le* = 3, *Sr* = 0.5%, ϕ = 2%, *N* = 1.75).

to high values of R_T, $R_T = 10^4$, 10^5 and 10^6, heat transfer first increases with particle volume fraction up to nearly (ϕ = 5% for $R_T = 10^4$, ϕ = 6% for $R_T = 10^5$, ϕ = 7% for $R_T = 10^6$) and then decreases with increasing particle fraction. Such a result for a 'homogeneous' fluid is considered as the reference, based on which we present the relative increase with the concentration for different R_T. The heat transfer increases with increasing particle volume fraction in a monotonic manner for low Rayleigh numbers because of the increase of the fluid thermal conductivity-as the heat transfer mechanism is mainly conduction.

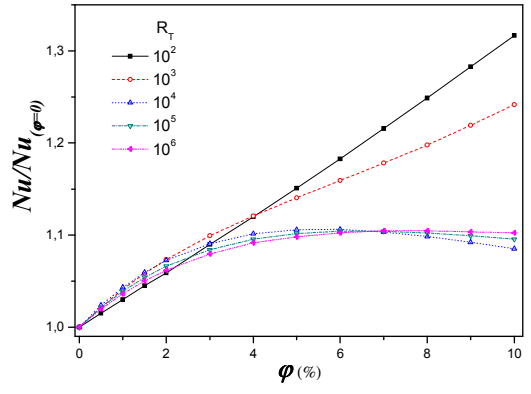

Figure 7 Effect of nanofluid concentration on relative heat transfer for different R_T (*a* = 1, *A* = 1, *Sr* = 2%, *Pr* = 6.2 and *Le* = 3).

It should be noted that the increase of heat transfer does not exceed 5%. It is worth mentioning that there exists a major difference between the cases of natural convection and forced convection as analysed by others authors, see for example [39]. Such a difference can be explained by the fact that in this study, the flow is not imposed, and hence appears to be more sensitive to a change of the fluid viscosity. The buoyancy strength is governed by the heating conditions imposed so that the intensity of the flow then decreases with increasing viscosity effect.

Nanoparticle type effect

Figure 8 presents the comparison of streamlines and isotherms using different nanofluids: TiO_2-water, Al_2O_3-water and Cu-water for $R_T = 10^4$. However, we varied the Rayleigh number for different types of nanoparticles, from diffusive state to convection state. For all nanofluids,

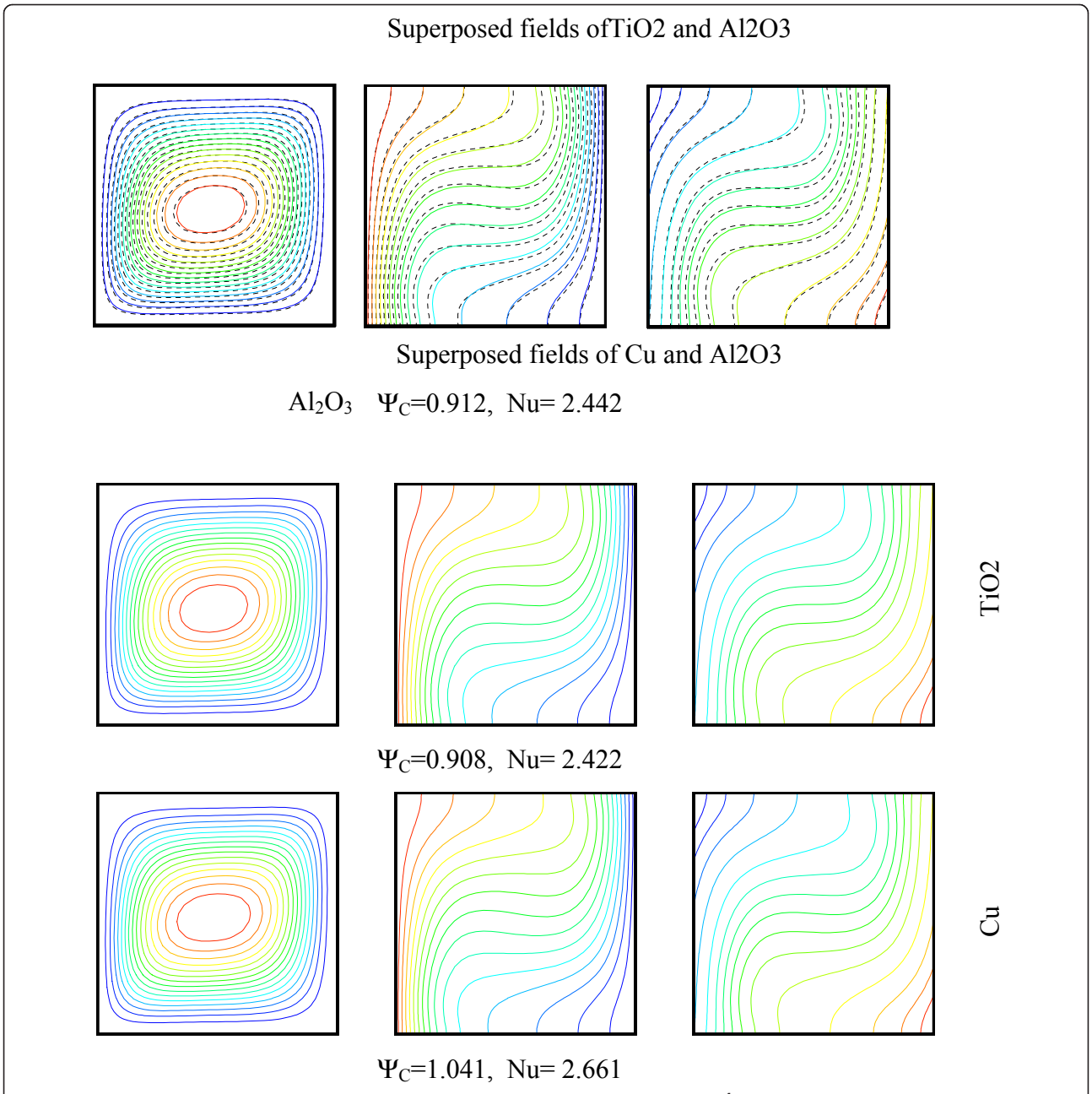

Figure 8 Dynamic, thermal and species fields for different nature of nanoparticle ($R_T = 10^4$, ϕ = 2%, *Pr* = 6.2, *Sr* = 2% and *Le* = 3).

a single cell movement was observed in a clockwise direction. The values of the maximum stream function show that the intensity of flow is higher for Cu-water than that of TiO_2-water and Al_2O_3-water. Hence, in the case of nanofluid heterogeneous solutal forces are in addition to heat one. The importance of solutal gradients, which differs from one type of nanofluid to another, directly affects the dynamic state and heat transfer (illustrated by figure 9 and 10). Indeed, Figure 11 presents the temperatures (a) and concentrations (b) in the middle horizontal plane of the square enclosure, for different nanofluids ($R_T = 10^4$, *Pr* = 6.2, *Le* = 3 and *Sr* = 2%), illustrates the distinction of each type. From superposed streamlines and isotherms of both TiO_2-water and Al_2O_3-water nanofluids, we find that the dynamic and thermal fields are similar. This reproaches qualitative aspects explained by the fact that the values of thermophysical properties of TiO_2-water and Al_2O_3-water are comparable. In opposition, this is not the case for the other two nanofluids Cu-water and Al_2O_3-water, which

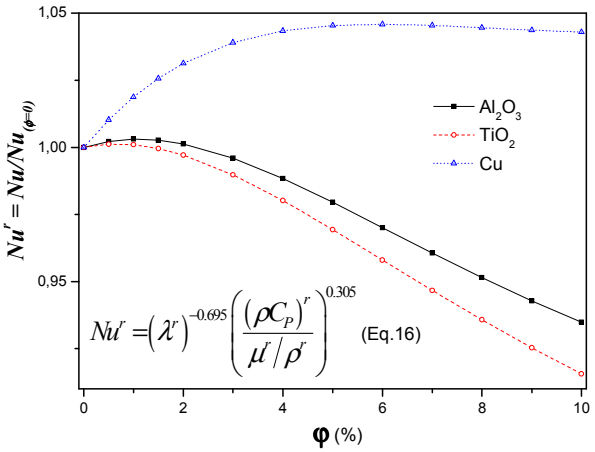

Figure 9 Nanoparticle fraction effect on heat transfer for different kind of particle: homogeneous case (a = 0, A = 1, $R_T = 10^5$).

the isotherms and the streamlines show that the distributions are very distinct.

Figure 9 shows the variation of relative Nusselt number, according to analytic approach (Equation 16) with volume fraction using different nanoparticles. We can note that the heat transfer increases with increasing the volume fraction for all nanofluids. For the three nanoparticles one notices the existence of a maximum, which is achieved by increasing the concentration, beyond which the transfer begins to decrease. This finding is valid for Al_2O_3-water and TiO_2-water but not for Cu-water. Indeed, the increase of thermophysical properties as a function of the nanoparticles, namely thermal conductivity, viscosity and specific heat capacity, affects the heat transfer and flow. So, increasing the viscosity with the nanoparticles is exacerbating the friction that causes a decrease in heat transfer. But in the case of Cu, which provides thermal conductivity and density that increases remarkably with the nanoparticles which outweighs the increase in the viscous effect and the specific heat capacity that decreases with the nanoparticles.

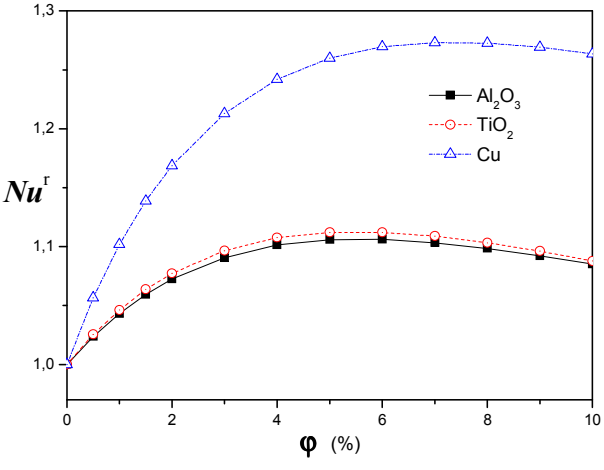

Figure 10 Effect of nature of nanoparticle on the nanofluid heat transfer: heterogeneous case ($R_T = 10^4$, Pr = 6.2, Sr = 2% and Le = 3).

We present on Figure 10 the variation of mean Nusselt number with volume fraction using different nanoparticles and different values of Rayleigh number. Results are presented for the case ($R_T = 10^4$, Pr = 6.2, Le = 3 and Sr = 2%). The figure shows that the heat transfer increases about monotonically with increasing the volume fraction for all Rayleigh numbers and nanofluids. For the three nanoparticles one notices the existence of a maximum, which is achieved by increasing the concentration, beyond which the transfer begins to decrease, but this maximum differs for Cu (7%), Al_2O_3 (6%) and TiO_2 (5%). The lowest heat transfer was obtained for TiO_2-water in view of the fact that TiO_2 has the lowest value of thermal conductivity compared to Cu and Al_2O_3. However, the difference in the values of Al_2O_3 and TiO_2 is negligible compared to the value of Cu. The thermal conductivity of TiO_2 is roughly one fifty of Cu. Yet, a unique property of Al_2O_3 is its high specific heat compared to Cu and TiO_2. The Cu nanoparticles have high values of thermal diffusivity and, thus, this reduces temperature gradients which will affect the performance of Cu nanoparticles. As volume fraction of nanoparticles increases, difference for mean Nusselt number becomes larger especially at higher Rayleigh numbers due to increasing of domination of convection mode of heat transfer. In fact, the temperature gradients grow to be more pronounced, which is illustrate in Figure 11a: the temperature along the middle plane of the square enclosure using different nanofluids for $Ra = 10^4$, Pr = 6.2, Le = 3 and Soret coefficient Sr = 2%.

The vertical velocity along the middle plane of the square enclosure using different nanofluids (for $R_T = 10^4$, Pr = 6.2, Le = 3 and Sr = 2%) is shown on Figure 12. Due to the floating flow inside the enclosure, the velocity shows a parabolic variation near the isothermal walls. The vertical velocity is susceptible to the nature of nanoparticles where two types of nanoparticles (Al_2O_3 and TiO_2) show similar vertical velocity but the third (Cu) is so different. This is explained in Equation 16 where the Brinkman formula shows that the viscosity of the nanofluid is only sensitive to the volume fraction of particles and not influenced by the type of nanoparticles and the expression of the buoyancy ration which is a function of the mass expansion coefficient that depends on the density of the nature of the particle. Indeed, the mass buoyancy force, in addition to the thermal buoyancy force, intensified the flow. Even then, the vertical velocity of

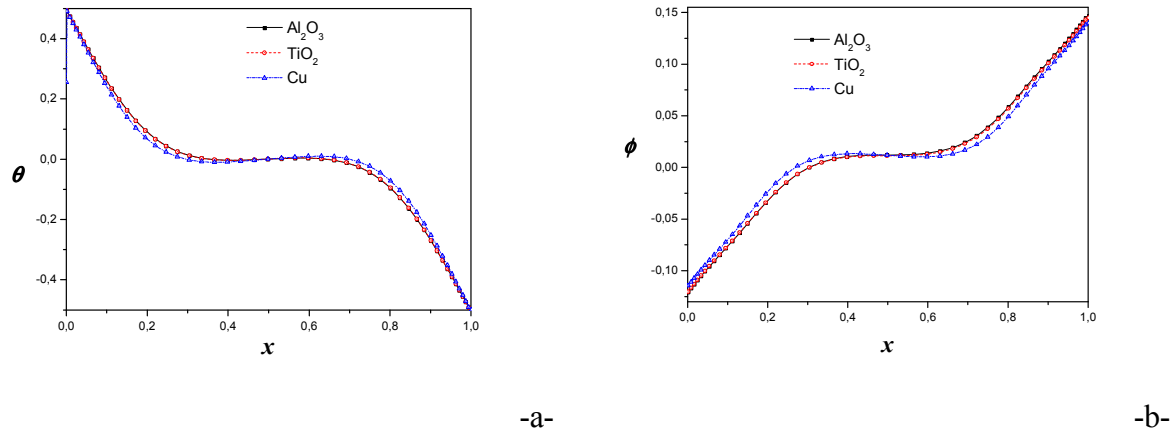

Figure 11 Temperature (a) and concentration (b) on the horizontal mid-plan (R_T = 10^4, ϕ = 2%, *Le* = 3 and *Sr* = 2%).

nanofluid is higher than that of pure fluid. It means that particle suspension affects the flow field. The flow velocity is almost zero around the centre of the cavity. The profile also gives idea on flow rotation direction.

Conclusion

The effect of using different nanofluids on the thermal and dynamic fields of natural convection in a differentially heated square cavity was studied numerically. Indeed, the results revealed that one type of nanofluid is a key factor for improving heat transfer. The highest values are obtained when using Cu nanoparticles. However, increasing the value of the Rayleigh number is growing the heat transfer. Moreover, the results show the influence due to competing effects between nanoparticles and thermal dynamics, and we identified the flow control parameters for different currents. The results also confirmed that the character of the natural convection directly affects a significant increase in heat transfer with the concentration of particles. Nevertheless the percentage of particle nature greatly affects the heat transfer and fluid flow.

The crossover Soret effect, which is the origin of the spatial distribution of nanoparticles concentrations, and its influence on heat transfer and flow field were studied. The percentage of the optimal nanoparticles concentration that maximises heat transfer was found and it is related to the kind of particle used.

The estimated Soret coefficient was supposed in this study not depending on the nanoparticles but we underline that molecular size and the electrical charges could modify the value of such coefficient and experimental work is necessary to go through this question.

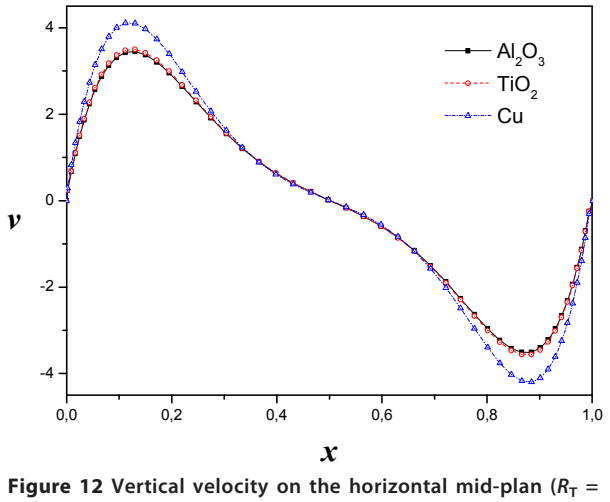

Figure 12 Vertical velocity on the horizontal mid-plan (R_T = 10^4, ϕ = 2%, *Le* = 3 and *Sr* = 2%).

Greek symbols

α: Thermal diffusivity, $\lambda/(\rho C_p)$; β_s: Solutal expansion coefficient; β_T: Thermal expansion coefficient; θ: Dimensionless temperature, = $\left(T^* - T_0^*\right)/\Delta T^*$; φ: Dimensionless concentration, = $\left(C^* - C_0^*\right)/\Delta C^*$; ϕ: Particle volume fraction; λ: Fluid thermal conductivity; μ: Dynamic viscosity; υ: Kinematic viscosity; ρ: Fluid density; Ψ: Stream function;

Superscripts

r: Nanofluid to base fluid ratio; *: Dimensional variable;

Subscripts

C: Center; S: Solutal; nf: Nanofluid; f: Base fluid; p: Particle; T: Temperature; 0: Reference state

Abbreviations

List of symbols

A: Aspect ratio of the enclosure, = *L*/*H*; *C*: Concentration; C_p: Specific heat; *D*: Mass diffusivity; D_T: Thermal mass diffusivity; *g*: Gravitational acceleration; *H*: Height of the enclosure; *L*: Width of the cavity; *Le*: Lewis number, = α/D; *N*:

Buoyancy ratio, $\beta_S \Delta C^*/\beta_T \Delta T^*$; *Nu*: Nusselt number, Equation 7; *p*: Dimensionless pressure, = $p^*H/\rho\alpha$; *Pr*: Prandtl number, υ/α; R_T: Thermal Rayleigh number, = $g\beta_T \Delta T^* H^3 \rho C_p/\upsilon\alpha$; R_s: Solutal Rayleigh number, = $g\beta_S \Delta S^* H^3 \rho C_p/\upsilon\lambda$; *Sc*: Schmidt nmber = υ/D; *Sh*: Sherwood number, Equation 7; S_r: Soret coefficient = D_T/D; ΔT^*: Characteristic temperature difference; ΔC^*: Characteristic concentration difference, $= -C_0^* (1 - C_0^*) \nabla T^* D_S / D$; (*x*, *y*): Dimensionless coordinate system, x^*/H, y^*/H; (*u*, *v*): Dimensionless velocity components, $u^*/(\upsilon/H)$, $v^*/(\upsilon/H)$.

Author details
[1]LETTM, Dept de physique, FST Campus Universitaire 2092 El Manar Tunis, Tunisie. [2]ENS-Cachan Dpt GC/LMT, 61, Av du Président Wilson 94235 Cachan Cedex, France.

Authors' contributions
FS carried out the numerical simulation studies, participated in the code modification and drafted the manuscript. RB carried out the code development and conceived of the study.

Competing interests
The authors declare that they have no competing interests.

Received: 3 December 2010 Accepted: 15 March 2011
Published: 15 March 2011

References

1. Hansen U, Yuen DA: **Subcritical double-diffusive convection at infinite Prandtl number.** *Geophys Astrophys Fluid Dyn* 1989, **47**:199-224.
2. Ostrach S: **Natural convection with combined driving forces.** *Physicochem Hydrodyn* 1980, **1(4)**:233-247.
3. Schmith RW: **Double diffusion in oceanography.** *Ann Rev Fluid Mech* 1994, **26**:255-236.
4. Turner JS: **Double-diffusive phenomena.** *Ann Rev Fluid Mech* 1974, **6**:37-56.
5. Nield DA: **The thermohaline Rayleigh-Jeffreys problem.** *J Fluid Mech* 1967, **29**:545-558.
6. Veronis G: **Effect of a stabilizing in thermohaline convection.** *J Fluid Mech* **34**:315-368.
7. Bennacer R, Mahidjiba A, Vasseur P, Beji H, Duval R: **The Soret effect on convection in a horizontal porous domain under cross temperature and concentration gradients.** *Int J Numer Methods Heat Fluid Flow* 2003, **13(2)**:199-215.
8. Ganguly S, Sikdar S, Basu S: **Experimental investigation of the effective electrical conductivity of aluminium oxide nanofluids.** *Powder Technol* 2009, **196**:326-330.
9. Merabia S, Shenogin S, Joly L, Keblinski P, Barrat J-L: **Heat transfer from nanoparticles: a corresponding state analysis.** *Proc Natl Acad Sci* 2009, **106(36)**:15113-15118.
10. Sefiane K, Bennacer R: **Nanofluids droplets evaporation kinetics and wetting dynamics on rough heated substrates.** *Adv Colloid Interface* 2009, **147-148**:263-271.
11. Anoop KB, Kabelac S, Sundararajan T, Das SK: **Rheological and flow characteristics of nanofluids: Influence of electroviscous effects and particle agglomeration.** *J Appl Phys* 2009, **106**:034909.
12. Bergman TL: **Effect of reduced specific heats of nanofluids on single phase, laminar internal forced convection.** *Int J Heat Mass Transf* 2009, **52**:1240-1244.
13. Lee J, Mudawar I: **Assessment of the effectiveness of nanofluids for singlephase heat transfer in micro-channels.** *Int J Heat Mass Transf* 2007, **50**:452-463.
14. Jain S, Patel HE, Das SK: **Brownian dynamic simulation for the prediction of effective thermal conductivity of nanofluid.** *J Nanopart Res* 2009, **11**:767-773.
15. Nelson IC, Banerjee D, Ponnappan R: **Flow loop experiments using polyalphaolefin.** *J Thermophys Heat Transf* 2009, **23**:752-761.
16. Namburu PK, Kulkarni DP, Dandekar A, Das DK: **Experimental investigation of viscosity and specific heat and silicon dioxide nanofluids.** *Micro Nano Lett* 2007, **2**:67-71.
17. Namburu PK, Kulkarni DP, Misra D, Das DK: **Viscosity of copper oxide nanoparticles dispersed in ethylene glycol and water mixture.** *Exp Therm Fluid Sci* 2007, **32**:397-402.
18. Vajjha RS, Das DK: **Specific heat measurement of three nanofluids and development of new correlations.** *ASME J Heat Transf* 2009, **131**:071601.
19. Zhou SQ, Ni R: **Measurement of the specific heat capacity of water-based AL2O3 nanofluid.** *Appl Phys Lett* 2009, **92**:093123.
20. Choi SUS: **Enhancing thermal conductivity of fluids with nanoparticles.** In *Developments and Applications of Non-Newtonian Flows, FED. Volume 231/ MD Volume 66.* Edited by: Siginer DA, Wang HP. New York: ASME; 1995:99-103.
21. Eastman SR, Phillpot S, Choi US, Keblinski P: **Thermal Transport in Nanofluids.** *Annu Rev Mater Res* 2004, **34**:219-46.
22. Maïga SE, Nguyen CT, Galanis N, Roy G: **Heat transfer enhancement in forced convection laminar tube flow by using nanofluids.** *Proc Int Symp Adv Comput Heat Transf CHT04, April 19-24; Norway* 2004.
23. Wang X, Mujumdar A: **Thermal characteristics of tree-shaped microchannel nets for cooling of a rectangular heat sink.** *Int J Therm Sci* 2006, **46(1)**:1-19.
24. Abu-Nada E: **Effects of variable viscosity and thermal conductivity of Al_2O_3-water nanofluid on heat transfer enhancement in natural convection.** *Int J Heat Mass Transfer* 2009, **30**:679-690.
25. Hwang KS, Jang SP, Choi SUS: **Flow and convective heat transfer characteristics of water-based Al2O3 nanofluids in fully developed laminar flow regime.** *Int J Heat Mass Transf* 2009, **52**:193-199.
26. Rea U, McKrell T, Hu L-W, Buongiorno J: **Laminar convective heat transfer and viscous pressure loss of alumina-water and zirconia-water nanofluids.** *Int J Heat Mass Transf* 2009, **52**:2042-2048.
27. Nield DA, Kuznetsov AV: **The onset of convection in a horizontal nanofluid layer of finite depth European.** *J Mech B/Fluids* 2010, **29**:217-223.
28. Bennacer R, El Ganaoui M, Maré T, Nguyen CT: **Natural convection of nanofluids in a cavity including Soret effect.** *Comput Therm Sci* 2009, **1(4)**:425-440.
29. Bennacer R, Mohamad AA, El Ganaoui M: **Thermodiffusion in porous media: Multidomain constituent separation.** *Int J Heat Mass Transf* 2009, **52**:1725-1733.
30. Pinheiro JP, Domingos R, Lopez R, Brayner R, Fiévet F, Wilkinson K: **Determination of diffusion coefficients of nanoparticles and humic substances using scanning stripping chronopotentiometry (SSCP).** *Colloids Surf A: Physicochem Eng Aspects* 2007, **295(1-3)**:200-208.
31. Ryskin A, Muller HW, Pleiner H: **Thermal convection in binary fluid mixtures with a weak concentration diffusivity, but strong solutal buoyancy forces.** *Phys Rev E* 2003, **67**:046302.
32. Choukairy K, Bennacer R, Vasseur P: **Natural convection in a vertical annulus boarded by an inner wall of finite thickness.** *Int Commun Heat Mass Transf* 2004, **31**:501-512.
33. De Vahl Davis G: **Natural convection in square cavity: a comparison exercise.** *Int J Numer Methods Fluids* 1983, **3**:227-248.
34. Drew DA, Passman SL: *Theory of Multicomponent Fluids* Berlin: Springer; 1999.
35. Brinkman HC: **The viscosity of concentrated suspensions and solution.** *J Chem Phys* 1952, **20**:571-581.
36. Keblinski P, Eastman JA, Cahill DG: **Nanofluids for thermal transport.** *Mater Today* 2005, 36-40.
37. Nguyen CT, Desgranges F, Galanis N, Roy G, Maré T, Boucher S, Mintsa HA: **Viscosity data for Al_2O_3-water nanofluid–hysteresis: is heat transfer enhancement using nanofluids reliable?** *Int J Therm Sci* 2008, **47**:103-111.
38. Hamilton RL, Crosser OK: **Thermal conductivity of heterogeneous two-component systems.** *I & EC Fundam* 1962, **1(3)**:187-191.
39. Akbarinia A, Behzadmehr A: **Numerical study of laminar mixed convection of a nanofluid in horizontal curved tubes.** *Appl Therm Eng* 2007, **27**:1327-1337.
40. Leal MA, Machado HA, Cotta RM: **Integral transform solutions of transient natural convection in enclosures with variable fluid properties.** *Int J Heat Mass Transf* 2007, **43**:3977-3990.
41. Sai BVKS, Seetharamu KN, Narayana PAA: **Solution of transient laminar natural convection in a square cavity by an explicit finite element scheme.** *Numer Heat Transf A* 1994, **25**:412-422.

doi:10.1186/1556-276X-6-222
Cite this article as: Oueslati and Bennacer: **Heterogeneous nanofluids: natural convection heat transfer enhancement.** *Nanoscale Research Letters* 2011 **6**:222.